

HEAVY-QUARK PRODUCTION IN $e\gamma$ SCATTERING

ERIC LAENEN

*CERN TH-Division
1211-CH, Geneva 23, Switzerland*

and

STEPHAN RIEMERSMA

*DESY - Zeuthen
Platanenallee 6, D-15735 Zeuthen, Germany***Abstract**

Open heavy flavour production at e^+e^- colliders in deeply inelastic $e\gamma$ scattering has an interesting feature: the structure function $F_2(x, Q^2)$ for this process is calculable for $x > 0.01$, and is essentially proportional to the gluon density in the photon for smaller x values. We give estimates for event rates at LEP2 and a Next Linear Collider in x, Q^2 bins, and present differential distributions in the transverse momentum and rapidity of the heavy quark for the case of charm. We include all next-to-leading-order QCD corrections, and find theoretical uncertainties are well under control.

1. Introduction

A copious amount of heavy quarks produced in two-photon collisions will be generated at high energy e^+e^- colliders such as LEP2 and a future Next Linear Collider (NLC). The largest fraction of these will come from so-called no-tag events, in which neither of the leptons generating the photons is seen. However, due to the high energy and luminosity of these machines, a sizeable number of them will be produced in events where either the outgoing e^+ or e^- is tagged (“single-tag events”). In such events, the photon coming from the tagged lepton is far off-shell and spacelike, hence this reaction amounts to deeply inelastic electroproduction of heavy quarks on a photon target. An important aspect of on-shell photons initiating a hard scattering is that they may behave either as pointlike particles (“direct” process), or as hadronic (vector) particles (“resolved” process) [1]. In no-tag events, both the direct and resolved process contribute to the cross section. At LEP2 they contribute in about equal amounts to the cross section for charm production in two-photon collisions [2]. In such events one can separate these components by making use of forward detectors and using the presence of a remnant jet of spectator partons in resolved processes as a separator [3]. The interesting feature of single-tag heavy-quark events is that this separation occurs quite naturally in the deeply inelastic Bjorken scaling variable x , as we will show below. Moreover, the presence of the heavy quark mass ensures that this separation is unambiguous to next-to-leading order (NLO) in QCD. The direct process is directly calculable in QCD and is free from such phenomenological inputs as parton densities in the photon. The resolved channel on the other hand is directly proportional to the poorly known gluon density in the photon. Therefore a reasonable sample of single-tag heavy-quark events allows one to confront simultaneously a well-controlled perturbative QCD calculation with experiment, and constrain the gluon density in the photon.

In the past (open) heavy quark (mainly charm) production in two-photon collisions at e^+e^- colliders has been difficult to observe in experiments due to the low charm acceptance. The reaction $e^+e^- \rightarrow e^+e^- D^{*\pm} X$ has been thoroughly studied experimentally. The existence of the $D^{*\pm}$ has been inferred either from direct reconstruction [4,5,6] or from unfolding the distribution of soft pions [7,8] resulting from its decay. In addition, measurements have been made using soft leptons [9,10] and kaons [3] to tag the charm. JADE [4] and TPC/Two-Gamma [5] have performed experimental studies of the reaction $e^+e^- \rightarrow e^+e^- D^{*\pm} X$ with one outgoing lepton tagged at low average value $\langle Q^2 \rangle$ of the momentum transfer squared of the tagged lepton (below 1 (GeV/c)²). TOPAZ [7] has performed a study as well at somewhat larger $\langle Q^2 \rangle$. The total number of events obtained was however very small (about 30 for TOPAZ). See [11] for a more extensive review of the experimental situation.

The cross section and single particle distributions for $\gamma\gamma \rightarrow c\bar{c}$ have been calculated to next-to-leading order (NLO) in QCD in [2], and agree with experimental results. Correlations in the direct channel were studied in [12]. For the single-tag case, the structure functions F_2^γ and F_L^γ for charm production were calculated to NLO in QCD in [13]. In this letter we employ the results of [13] to estimate the expected number of single-tag events in x, Q^2 bins for LEP2 and a NLC, and examine differential distributions in the transverse

momentum and rapidity of the charm quark.

In section 2 we describe the formalism and explain our notation. In section 3 we show the structure function F_2^γ for charm production, give estimates of event rates in x, Q^2 bins for the case of LEP2 and a NLC and show single-charm-quark differential distributions. We summarize and conclude in section 4.

2. Formalism

We consider the reaction (see Fig.1)

$$e^-(p_e) + e^+ \rightarrow e^-(p_e') + e^+ + Q(p_1) + X, \quad (1)$$

where $Q(p_1)$ is a heavy quark with momentum p_1 and X denotes any hadronic state allowed by quantum-number conservation laws. When the outgoing electron is tagged, this reaction

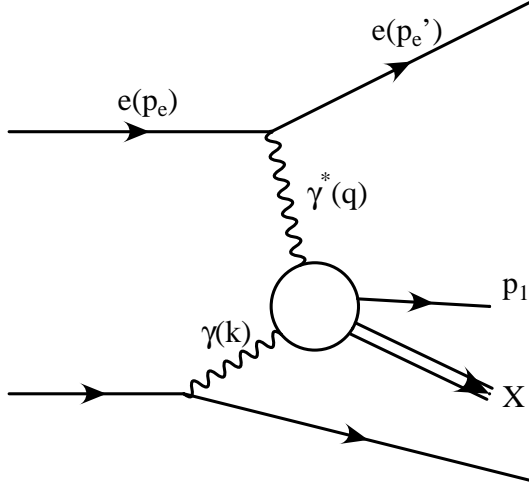


Figure 1: *Charm production in a single-tag two-photon event.*

is dominated by the subprocess

$$\gamma^*(q) + \gamma(k) \rightarrow Q(p_1) + X, \quad (2)$$

where one of the photons is highly virtual and the other is almost on-mass-shell and transversely polarized. The case where the positron is tagged is completely equivalent. This process is described by the differential cross section

$$\begin{aligned} \frac{d^4\sigma}{dx dQ^2 dT_1 dU_1} &= \int dz f_\gamma^e(z, \frac{S}{m_e^2}) \frac{2\pi\alpha^2}{x Q^4} \\ &\times \left[(1 + (1-y)^2) \frac{d^2 F_2^\gamma(x, Q^2, m^2)}{dT_1 dU_1} - y^2 \frac{d^2 F_L^\gamma(x, Q^2, m^2)}{dT_1 dU_1} \right], \end{aligned} \quad (3)$$

where the $d^2 F_k^\gamma(x, Q^2, m^2)/dT_1 dU_1$ ($k = 2, L$) denote the (doubly differential) deeply inelastic photon structure functions, $\alpha = e^2/4\pi$ is the fine structure constant, and m the

heavy quark mass. S is the center of mass energy squared of the e^+e^- system. The Bjorken scaling variables x and y are defined by

$$x = \frac{Q^2}{2k \cdot q}, \quad y = \frac{k \cdot q}{k \cdot p_e}, \quad q = p_e - p'_e. \quad (4)$$

Further, we define the variables

$$T_1 = T - m^2 = (k - p_1)^2 - m^2, \quad U_1 = U - m^2 = (q - p_1)^2 - m^2. \quad (5)$$

The momenta of the off-shell photon and the on-shell photon obey the relations $q^2 = -Q^2 < 0$ and $k^2 \approx 0$ respectively. Because the photon with momentum k is almost on-mass-shell, eq. (3) is written in the Weizsäcker-Williams approximation: the function $f_\gamma^e(z, S/m_e^2)$ represents the probability of finding a photon $\gamma(k)$ in the positron, with longitudinal momentum fraction z . It is given by [14]

$$f_\gamma^e(z) = \frac{\alpha}{2\pi} \left\{ \frac{1 + (1-z)^2}{z} \ln \frac{k_{\max}^2}{k_{\min}^2} - 2m_e^2 z \left(\frac{1}{k_{\min}^2} - \frac{1}{k_{\max}^2} \right) \right\}, \quad (6)$$

where $k_{\min}^2 = (z^2 m_e^2)/(1-z)$ and $k_{\max}^2 = (1-z)(E_b \theta_{\max})^2 + (z^2 m_e^2)/(1-z)$. Here $E_b = \sqrt{S}/2$ is the lepton beam energy and θ_{\max} is the anti-tag¹ angle. In the rest of the calculation $k^2 = 0$.

In eq. (3) the differential structure functions can be represented as

$$\begin{aligned} dF_k^\gamma(x, Q^2, m^2) &= dC_{k,\gamma}(x, \frac{Q^2}{m^2}) + \sum_{i=q,\bar{q},g} \int_x^{z_{\max}} \frac{dz}{z} f_i^\gamma(\frac{x}{z}, \mu_f^2) dC_{k,i}(z, \frac{Q^2}{\mu_f^2}, m^2) \\ &= dF_k^{\gamma,PL} + dF_k^{\gamma,HAD}, \end{aligned} \quad (7)$$

where d represents $d^2/dT_1 dU_1$ and $z_{\max} = Q^2/(Q^2 + 4m^2)$. The two terms represent the contributions to the structure functions from pointlike (or “direct”) and hadronic (or “resolved”) photons, respectively. The f_i^γ are photonic parton densities and the $dC_{k,i}$ ($i = q, \bar{q}, g, \gamma$) are (differential) Wilson coefficient functions, and μ_f is the mass factorization scale. At lowest order, only the photonic gluon density appears in eq. (7). F_2^γ and F_L^γ were calculated in [13] to NLO in QCD by computing all $O(\alpha_s)$ corrections to the coefficient functions $C_{k,i}$. We use the results of this calculation for the present analysis. Coupling constant renormalization was performed in the $\overline{\text{MS}}$ scheme, modified such that heavy flavours decouple in loops when small momenta flow into the fermion loop, and mass renormalization in the on-shell scheme. Mass factorization was also performed in the $\overline{\text{MS}}$ scheme. See [13] for further details. Note the absence of the scale μ_f in the second term on the right hand side of eq. (7). This is due to the fact that, through NLO, the heavy quark mass prevents a collinear singularity from occurring in the pointlike piece. For massless quarks this singularity is subtracted at scale μ_f and absorbed into the hadronic piece. As a consequence $F_k^{\gamma,PL}$ is calculable – the only theoretical uncertainties stemming from α_s and the heavy quark mass – whereas $F_k^{\gamma,HAD}$ is primarily sensitive to the gluon density in the photon, in

¹The maximum angle below which no energy deposit in forward calorimeters may be seen, thus selecting events in which the lepton generating the target photon goes down the beampipe.

analogy to the proton case. We will see that the two components on the right hand side in eq. (7) dominate in different regions of the Bjorken variable x . From eq. (3) we will estimate the numbers of events expected per x, Q^2 bin at LEP2 and a future NLC.

In analyzing charm production, we will also show differential distributions in transverse momentum and rapidity of the detected charm quark in the γ^*e^+ c.m. frame. These quantities are derived from the variables defined in the above as follows. We define W to be the invariant mass squared

$$W = (q + k)^2 \quad (8)$$

and $W' = W + Q^2$. The transverse mass of the heavy quark in the $\gamma^*\gamma$ frame is determined by

$$W'^2 m_T^2 = W' T_1 U_1 + Q^2 T_1^2 + Q^2 W' T_1. \quad (9)$$

The transverse mass is the same in the γ^*e^+ frame. Further, in the $\gamma^*\gamma$ frame the energy of the heavy quark is

$$\tilde{E} = \frac{-Q^2 - T_1 - U_1}{2\sqrt{W}}. \quad (10)$$

Its longitudinal momentum can be found from the condition $\tilde{P}_L^2 = \tilde{E}^2 - m_T^2$, so its rapidity in the $\gamma^*\gamma$ frame is

$$\tilde{y} = \frac{1}{2} \ln \left(\frac{\tilde{E} + \tilde{P}_L}{\tilde{E} - \tilde{P}_L} \right). \quad (11)$$

In the γ^*e^+ frame, $y = \tilde{y} + \frac{1}{2} \ln(z)$ (we define a particle to have positive rapidity when it travels into the hemisphere from which the γ^* originates).

3. Results

We first list our choices for various quantities used in the calculations of this section. Deviations from them will be explicitly indicated. We used for m , the heavy quark mass, the value 1.5 GeV for charm and 4.75 GeV for bottom. We assumed a center of mass energy $\sqrt{S} = 180$ (500) GeV for LEP2 (NLC). For the strong coupling we took a one-loop running α_s with three (four) light flavours and $\Lambda = 232$ (200) MeV at LO and a two-loop running α_s with $\Lambda = 248$ (200) MeV at NLO for charm (bottom). We put the renormalization scale equal to the factorization μ_f and chose $\mu_f = Q$. We also imposed the following requirements on the angle and energy of the tagged lepton: $\theta_{\text{tag}} > 30$ (40) mrad for LEP2 (NLC) and $E_{\text{tag}} > E_{\text{beam}}/2$, where $E_{\text{beam}} = \sqrt{S}/2$. These cuts imply a minimum Q^2 of 3.65 GeV² for LEP2 and 50 GeV² at our hypothetical NLC. Furthermore we used the GRV [15] parton densities for the hadronic photon results, and the Weizsäcker-Williams density of [14] with a $\theta_{\text{max}} = \theta_{\text{tag}}$ for the equivalent target photon spectrum. For the total integrated luminosity of LEP2 (NLC) we used $\int \mathcal{L} dt = 500 \text{ pb}^{-1}$ (20 fb⁻¹). At a NLC, beamstrahlung effects are expected to play an important rôle. We include them here by adopting for its spectrum the expression given in [19], with parameters $\Upsilon_{eff} = 0.039$ and $\sigma_z = 0.5$ mm [20], corresponding to the TESLA design. When showing differential distributions we will show them from the point of view of the γ^*e^+ cm frame, *i.e.* we assume here that the electron is tagged and

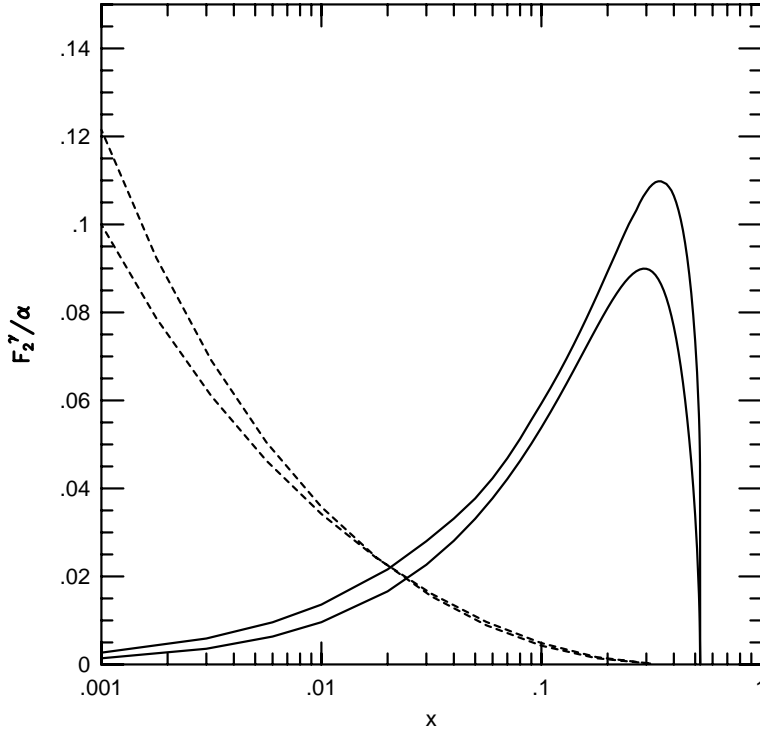


Figure 2: *Hadronic (dashed lines) and pointlike (solid lines) components of F_2^γ/α vs. x at $Q^2 = 10 \text{ (GeV/c)}^2$. The lower solid line is the LO, the upper one the NLO case. The lower dashed line at $x = 0.001$ is the NLO, the upper one the LO case.*

take the case where the positron is tagged into account by multiplying the results with a factor 2.

We begin by showing in Fig.2 the quantities $F_2^{\gamma,PL}$ and $F_2^{\gamma,HAD}$ versus x both at LO and NLO, for $Q^2 = 10 \text{ (GeV/c)}^2$. The $O(\alpha_s)$ corrections to both quantities are for the most part fairly small in the x -region shown. We may therefore assume that even higher order contributions are negligible, and these components are thus calculated with some accuracy.

The prominent feature in these figures is clearly the separation in x of the components. This fact was already noted in [13], and we emphasize it here. As a result, the opportunity to confront a precise calculation and measure the small- x photonic gluon density presents itself in one experiment. As mentioned earlier, the difficulty of efficient charm tagging makes such an experimental study very difficult in practice. To judge the feasibility of such a study we have integrated eq. (3) for various x, Q^2 bins, and obtained estimates for the number of charm quarks per bin produced at LEP2 and NLC by both hadronic and pointlike photons. Note that these estimates use the NLO calculation.

To perform the integrals over x and Q^2 , we used fitted versions of the *integrated* NLO coefficient functions $C_{k,i}$ ($i = q, \bar{q}, g, \gamma$) in eq. (7), as the actual expressions in [13] are too long for fast evaluation. By adapting the fitted coefficient functions of electroproduction of heavy quarks on a proton target [17] to the photon target, we were able to speed up our computer program by as much as a factor of fifty.

The results for LEP2 are shown in Tables 1 and 2. We give in these tables the expected number of events due to pointlike (Table 1) and hadronic (Table 2) photons. Assuming a

charm tagging efficiency of 1-2%, we that on average a few tens of events per bin should be observable for larger x values. Furthermore, to test the stability of the results we varied the renormalization/factorization scale μ_f from $Q/2$ to $2Q$. The results change relatively little under these variations, as seen in Tables 1 and 2. For these LEP2 conditions, we varied in addition the charm quark mass from 1.3 GeV to 1.7 GeV and found that the pointlike contribution (Table 1) changed under this variation in the charm mass by less than 10% in all bins, except in the x bins $0.32 < x < 1$. In these bins, the mass variation causes a variation in the position of the charm quark production threshold, and from the shape of $F_2^{\gamma, PL}$ in Fig.2 one may readily understand that this causes a large change in the number of events, as much as 70% in the lowest Q^2 bin. The sensitivity of the hadronic contribution (Table 2) to these changes is much more uniform in x , varying from 30-40% in the lowest Q^2 bin to 10-20% in the higher Q^2 bins.

In Table 3 we give similar estimates for the NLC, both for charm and bottom production. Here we have summed the contributions due to pointlike and hadronic photons for each entry. We do however show separately the number of events due to beamstrahlung and Weizsäcker-Williams bremsstrahlung contributions. Note that the number of charmed events here is truly large, even at large Q^2 . The number of events containing bottom quarks is much smaller due to charge and phase space suppression.

Clearly the production rate of charm quarks produced by hadronic photons is too small at LEP2 to be useful for a good measurement of the gluon density in the photon. At a NLC the rates are significantly higher however. We therefore give in Table 4 the production rate for a NLC in x, Q^2 bins for various choices of parton densities, charm quark mass values and mass factorization scales. Examining the composition of these results, we find very little contribution due to the hadronic channel from beamstrahlung photons (about 1-2%). We further find the contributions due to pointlike photons both of WW and beamstrahlung origin to be similarly small. There is therefore a good possibility of measuring the gluon density in the photon at a NLC, poor tagging efficiency notwithstanding. The most significant uncertainty is related to the charm quark mass, however a differentiation of the gluon densities of GRV [15] and ACFGP [16] seems certainly feasible.

While bottom quark production lends itself to considerably better tagging efficiencies, the production rate is severely suppressed relative to charm. An analysis similar to the one for charm reveals that a measurement of the photonic gluon density from bottom production in $e\gamma$ scattering does not seem possible at a NLC.

We turn to single particle inclusive differential distributions in transverse momentum (p_t) and rapidity (y) of the heavy quark in the γ^*e^+ c.m. frame. Due to the low rate of bottom quark production we only show these distributions for the case of charm. We integrate x and Q^2 over the intervals $0.001 < x < 1$ and $3.2 < Q^2 < 320$ (3200) GeV^2 for LEP2 (NLC). To approximate detector limitations, we use the restrictions $p_t > 0.5$ GeV and $|y| < 2$, in addition to the cuts listed in the beginning of this section. The p_t restriction is of course quite loose, but it allows us to study the behavior of the p_t spectrum at low p_t . Furthermore, for the results shown in Figs.3 and 4 we took the factorization (=renormalization) scale $\mu_f = \sqrt{Q^2 + p_t^2}$.

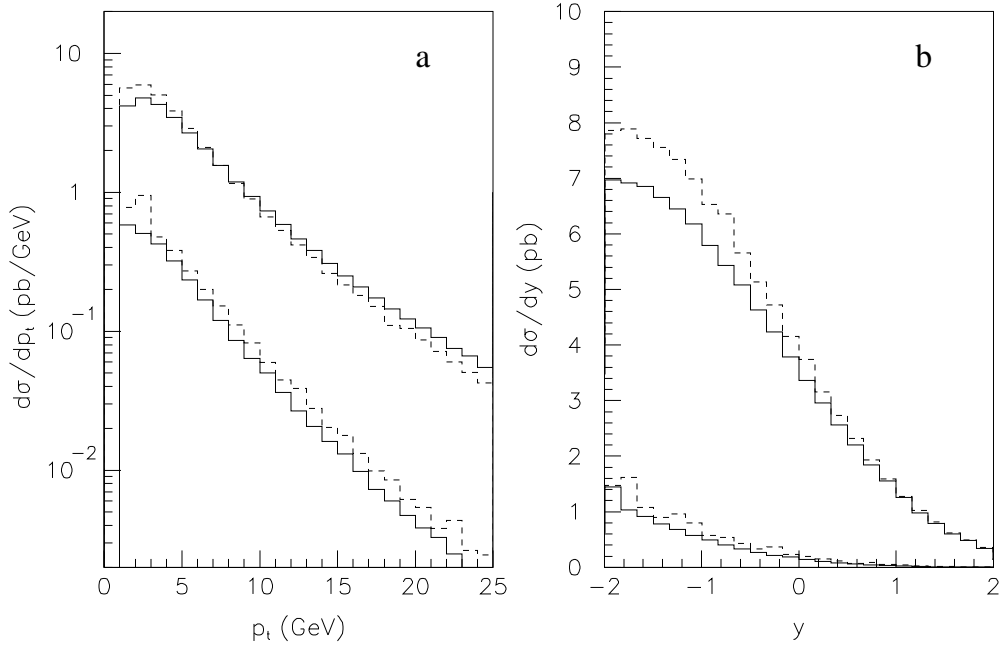


Figure 3: *Hadronic and pointlike distributions in p_t and y of the charm quark in LO and NLO at LEP2. a) The upper set of histograms represents the pointlike p_t -distribution, the lower the hadronic. The solid histograms represent the LO case, the dashed the NLO. b) Same as in a) but now for the y -distribution.*

In Fig.3a we present for LEP2 the LO and NLO p_t -distributions of the charm quark for the pointlike and hadronic piece separately. In neither instance do the LO and NLO curves differ significantly. While the hadronic piece at NLO is larger than the LO at large p_t (which is similar to what was found for a proton target in [21]), the reverse is true for the pointlike piece. The bulk of the events has $p_t < 5$ GeV. In Fig.3b the same is shown but now for the rapidity distribution. Clearly the charm quark has predominantly negative rapidity.

In Figs.4a and 4b we present for the NLC the p_t spectrum results due to pointlike and hadronic photons for a Weizsäcker-Williams spectrum and a beamstrahlung photon spectrum. Both spectra lead to similar plots as for LEP2 in Fig.3a. The dominance near small p_t of the beamstrahlung piece is due to the small final-state invariant mass preferred by the beamstrahlung spectrum.

4. Conclusions

We have argued in this letter that a measurement of the cross section for heavy quark production in single-tag two-photon events is interesting, because it enables one to compare a well-controlled QCD calculation with data at large x and constrain the gluon content of the photon at small x .

Both in the p_t and y distributions very little distinguishes the NLO results from the LO.

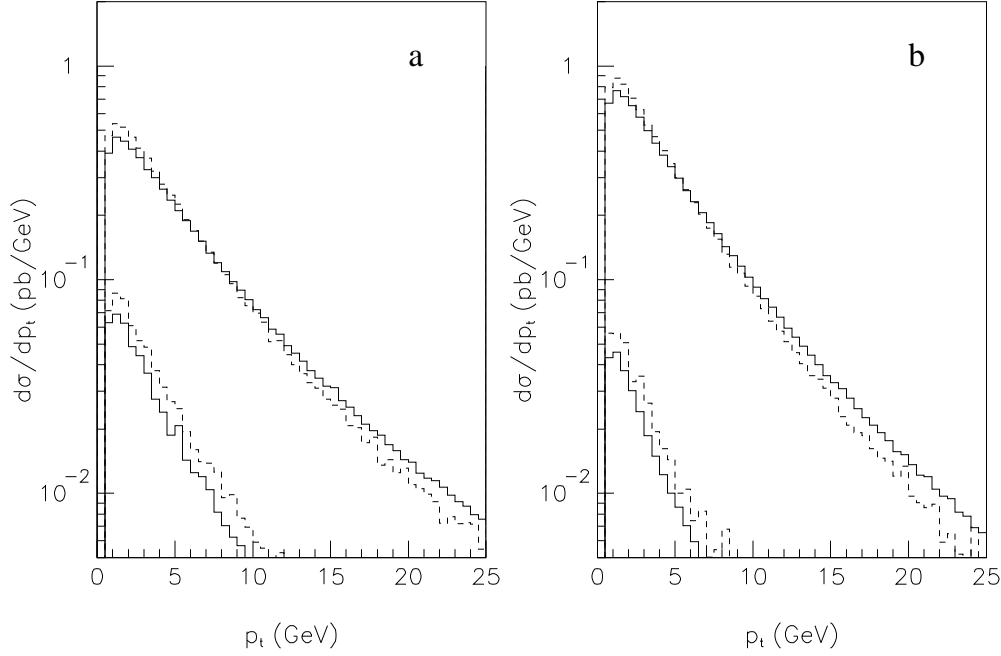


Figure 4: *Hadronic and pointlike distributions in p_t of the charm quark in NLO for the Weizsäcker-Williams (WW) and beamstrahlung cases at a NLC. a) WW case. The upper set of histograms is the pointlike component, the lower the hadronic. The solid histograms represent the LO case, the dashed ones the NLO case. b) Same as in a) but now for the (TESLA) beamstrahlung spectrum.*

Assuming a not overly pessimistic charm acceptance, a measurement of the pointlike structure function seems feasible at LEP2, and both the pointlike and hadronic structure functions are certainly measurable at a future NLC.

References

- [1] T.F. Walsh and P.M. Zerwas, Phys. Lett. **B44** (1973) 195; E. Witten, Nucl. Phys. **B120** (1977) 189.
- [2] M. Drees, M. Krämer, J. Zunft and P. Zerwas, Phys. Lett. **B306** (1993) 371.
- [3] R. Enomoto et al. (TOPAZ), Phys. Lett. **B341** (1994) 238.
- [4] W. Bartel et al. (JADE), Phys. Lett. **B184** (1987) 288; A.J. Finch in Proceedings of the VIII International Workshop on Photon-Photon Collisions, Shresh, Israel (1988), U. Karshon ed. (World Scientific), p75.
- [5] M. Alston-Garnjost et al. (TPC/Two-Gamma), Phys. Lett. **B252** (1990) 499.
- [6] W. Braunschweig et al. (TASSO), Z. Phys. **C47** (1990) 499; R. Enomoto et al. (TOPAZ), Phys. Rev. **D50** (1994) 1879; D. Buskulic et al. (ALEPH), Phys. Lett. **B355** (1995) 595.

- [7] R. Enomoto et al. (TOPAZ), Phys. Lett. **B328** (1994) 535.
- [8] T. Nozaki (AMY collab.) in Proceedings of Photon'95, Sheffield (1995), S. Cartwright and D. Miller eds. (World Scientific).
- [9] T. Nozaki (AMY) in Proceedings of Photon'95, Sheffield (1995), S. Cartwright and D. Miller eds. (World Scientific); S. Uehara et al. (VENUS), Z. Phys. **C63** (1994) 213;
- [10] R. Enomoto et al. (TOPAZ), Phys. Lett. **B341** (1994) 99.
- [11] P. Aurenche et al., $\gamma\gamma$ *Physics*, in: Proceedings of the Workshop *Physics with LEP2*, eds. G. Altarelli and F. Zwirner, CERN 1995.
- [12] M. Krämer and E. Laenen, preprint CERN-TH/95-291, DESY 95-199, to be published in Phys. Lett. B.
- [13] E. Laenen, S. Riemersma, J. Smith and W.L. van Neerven, Phys. Rev. **D49** (1994) 5753.
- [14] S. Frixione, M. Mangano, P. Nason and G. Ridolfi, Phys. Lett. **B319** (1993) 339.
- [15] M. Glück, E. Reya and A. Vogt, Phys. Rev. **D46** (1992) 1973.
- [16] P. Aurenche, P. Chiapetta, M. Fontannaz, J.Ph. Guillet and E. Pilon, Z. Phys. **C56** (1992) 589; P. Aurenche, J.-P. Guillet and M. Fontannaz, Z. Phys. **C64** (1994) 621.
- [17] S. Riemersma, J. Smith and W.L. van Neerven, Phys. Lett. **B347** (1995) 143.
- [18] T. Nozaki, in Proceedings of Photon'95, Sheffield (1995), S. Cartwright and D. Miller eds. (World Scientific). M. Iwasaki, ibidem. F. Foster, ibidem.
- [19] P. Chen, T. Barklow and M.E. Peskin, Phys. Rev. **D49** (1994) 3209.
- [20] D. Schulte, private communication.
- [21] E. Laenen, S. Riemersma, J. Smith and W.L. van Neerven, Nucl. Phys. **B392** (1993) 229.

Q^2	x	Events		
range	range	$\mu_f = Q/2$	$\mu_f = Q$	$\mu_f = 2Q$
3.2 - 10	$3.2 - 10.0 \cdot 10^{-4}$	3	2	2
	$1.0 - 3.2 \cdot 10^{-3}$	25	21	20
	$3.2 - 10.0 \cdot 10^{-3}$	106	94	88
	$1.0 - 3.2 \cdot 10^{-2}$	339	314	296
	$3.2 - 10.0 \cdot 10^{-2}$	919	884	857
	$1.0 - 3.2 \cdot 10^{-1}$	2350	2220	2180
	$3.2 - 10.0 \cdot 10^{-1}$	1040	916	845
10 - 32	$1.0 - 3.2 \cdot 10^{-3}$	7	6	6
	$3.2 - 10.0 \cdot 10^{-3}$	63	58	55
	$1.0 - 3.2 \cdot 10^{-2}$	294	276	266
	$3.2 - 10.0 \cdot 10^{-2}$	999	968	951
	$1.0 - 3.2 \cdot 10^{-1}$	2910	2860	2830
	$3.2 - 10.0 \cdot 10^{-1}$	3040	2880	2780
32 - 100	$3.2 - 10.0 \cdot 10^{-3}$	6	6	5
	$1.0 - 3.2 \cdot 10^{-2}$	54	51	50
	$3.2 - 10.0 \cdot 10^{-2}$	248	241	235
	$1.0 - 3.2 \cdot 10^{-1}$	825	814	808
	$3.2 - 10.0 \cdot 10^{-1}$	1550	1520	1500
100 - 320	$1.0 - 3.2 \cdot 10^{-2}$	5	5	5
	$3.2 - 10.0 \cdot 10^{-2}$	45	44	43
	$1.0 - 3.2 \cdot 10^{-1}$	196	194	193
	$3.2 - 10.0 \cdot 10^{-1}$	511	509	508

Table 1: Number of events with charm quarks due to pointlike photons at LEP2 in $e\gamma$ collisions.

Q^2	x	Events		
range	range	$\mu_f = Q/2$	$\mu_f = Q$	$\mu_f = 2Q$
3.2 - 10	$3.2 - 10.0 \cdot 10^{-4}$	94	86	86
	$1.0 - 3.2 \cdot 10^{-3}$	299	275	266
	$3.2 - 10.0 \cdot 10^{-3}$	379	342	328
	$1.0 - 3.2 \cdot 10^{-2}$	328	290	271
	$3.2 - 10.0 \cdot 10^{-2}$	192	159	144
	$1.0 - 3.2 \cdot 10^{-1}$	53	36	30
	$3.2 - 10.0 \cdot 10^{-1}$	1	0	0
10 - 32	$1.0 - 3.2 \cdot 10^{-3}$	121	116	116
	$3.2 - 10.0 \cdot 10^{-3}$	333	320	313
	$1.0 - 3.2 \cdot 10^{-2}$	410	385	372
	$3.2 - 10.0 \cdot 10^{-2}$	306	279	267
	$1.0 - 3.2 \cdot 10^{-1}$	111	95	88
	$3.2 - 10.0 \cdot 10^{-1}$	5	3	3
32 - 100	$3.2 - 10.0 \cdot 10^{-3}$	44	45	45
	$1.0 - 3.2 \cdot 10^{-2}$	109	108	108
	$3.2 - 10.0 \cdot 10^{-2}$	112	110	110
	$1.0 - 3.2 \cdot 10^{-1}$	55	54	54
	$3.2 - 10.0 \cdot 10^{-1}$	5	5	6
100 - 320	$1.0 - 3.2 \cdot 10^{-2}$	11	11	12
	$3.2 - 10.0 \cdot 10^{-2}$	23	24	24
	$1.0 - 3.2 \cdot 10^{-1}$	16	17	18
	$3.2 - 10.0 \cdot 10^{-1}$	3	3	3

Table 2: Number of events with charm quarks due to hadronic photons at LEP2 in $e\gamma$ collisions.

Q^2	x	Events			
range	range	$c(\text{WW})$	$b(\text{WW})$	$c(\text{Beam})$	$b(\text{Beam})$
32 - 100	$1.0 - 3.2 \cdot 10^{-3}$	1850	120	30	2
	$3.2 - 10.0 \cdot 10^{-3}$	2460	150	1170	70
	$1.0 - 3.2 \cdot 10^{-2}$	2420	130	4060	200
	$3.2 - 10.0 \cdot 10^{-2}$	2780	110	6510	260
	$1.0 - 3.2 \cdot 10^{-1}$	4470	150	9590	320
	$3.2 - 10.0 \cdot 10^{-1}$	6740	60	11,300	110
100 - 320	$1.0 - 3.2 \cdot 10^{-3}$	1040	80	0	0
	$3.2 - 10.0 \cdot 10^{-3}$	3790	300	220	20
	$1.0 - 3.2 \cdot 10^{-2}$	6230	430	3150	200
	$3.2 - 10.0 \cdot 10^{-2}$	10,300	510	12,200	580
	$1.0 - 3.2 \cdot 10^{-1}$	21,700	830	34,700	1320
	$3.2 - 10.0 \cdot 10^{-1}$	43,300	730	73,800	1240
320 - 1000	$1.0 - 3.2 \cdot 10^{-2}$	1050	110	70	10
	$3.2 - 10.0 \cdot 10^{-2}$	2310	160	1230	80
	$1.0 - 3.2 \cdot 10^{-1}$	5610	260	6790	310
	$3.2 - 10.0 \cdot 10^{-1}$	13,300	400	21,200	620
1000 - 3200	$1.0 - 3.2 \cdot 10^{-2}$	70	10	0	0
	$3.2 - 10.0 \cdot 10^{-2}$	370	30	30	2
	$1.0 - 3.2 \cdot 10^{-1}$	1210	70	670	10
	$3.2 - 10.0 \cdot 10^{-1}$	3480	140	4200	160

Table 3: Number of events with charm and bottom quarks at a NLC in $e\gamma$ collisions.

Charm Mass	Q^2 range	x range	Events		
			$\mu_f = Q/2$	$\mu_f = Q$	$\mu_f = 2Q$
1.3	32 - 100	$1.0 - 3.2 \cdot 10^{-3}$	2080	2140	2230
1.5			1880	1890	1930
1.7			1740	1750	1790
1.3	32 - 100	$3.2 - 10.0 \cdot 10^{-4}$	346	356	370
1.5			317	322	329
1.7			296	305	313
1.3	100 - 320	$1.0 - 3.2 \cdot 10^{-3}$	1060	1100	1140
1.5			987	1024	1058
1.7			907	930	954
1.3	32 - 100	$1.0 - 3.2 \cdot 10^{-3}$	3770	4080	4500
1.5			3490	3740	4090
1.7			3240	3480	3810
1.3	32 - 100	$3.2 - 10.0 \cdot 10^{-4}$	478	509	561
1.5			449	480	531
1.7			419	452	502
1.3	100 - 320	$1.0 - 3.2 \cdot 10^{-3}$	829	916	1010
1.5			774	854	943
1.7			716	777	847

Table 4: Number of events with charm at small x at a NLC in $e\gamma$ collisions. We used GRV [15] $\overline{\text{MS}}$ parton distributions for the top half and ACFGF [16] ones for the bottom half.